Evaluation for Laser Command Generation in Directed Energy Deposition Applying a Three Dimensional Heat Conduction Simulation

Toshiki Kodama[1, a], Ryo Koike[1, b*], Yasuhiro Kakinuma[1, c], and Yohei Oda[2, d]

[1] Department of System Design Engineering, Keio University, Japan

[2] DMG Mori Co., Ltd., Japan

[a]kodama@ams.sd.keio.ac.jp, [b] koike@sd.keio.ac.jp, [c] kakinuma@sd.keio.ac.jp, [d] yo-oda@dmgmori.co.jp

Keywords: Additive manufacturing, Directed energy deposition, Heat conduction simulation, Inconel 625, thermography

Abstract. Metal additive manufacturing is a promising process for various industries in next generation, which provides high freedom of design, waste reduction, and applicability to difficult-to-cut materials. Directed energy deposition, which is one method of metal additive manufacturing, still has a challenge in the shape accuracy which deteriorates due to overheating in the edge. In order to suppress the overheating, this study proposes a laser command generation available to each deposition path by applying a heat conduction simulation. The laser command is determined by a three-dimensional heat conduction simulation with a finite difference method. The proposed laser command generation was evaluated through the deposition test, comparing with a conventional process with constant laser power. The experimental result clearly shows that the deformation due to overheating can be suppressed by adjusting the laser power according to the deposition height. Moreover, through the temperature measurement with a thermography, and calibrating the simulation, the deterioration in shape accuracy can be efficiently suppressed.

Introduction

Additive manufacturing (AM) is defined by ISO 17296 and ASTM F2792 to be the process of joining materials to make parts or objects from 3D model data, usually layer upon layer, as opposed to subtractive manufacturing methodologies [1]. Industries recently have paid much attention on the AM because of its applicability of the production of difficult-to-cut material with small amount of waste and cost. In addition, the AM is a promising approach to high-mix low-volume production by forming various shapes without any molds.

AM is no longer a proto-type manufacturing but a sophisticated solution adaptive to various materials such as metals, polymers, ceramics, and biological materials [2]. In the light of metals, powder bed fusion (PBD) and directed energy deposition (DED) are efficient approaches to deposit a high-volume production in heavy industries like aerospace and automobile. In particular, DED achieves higher efficiency than PBD by melting and solidifying large amount of powder material with a high-power heat source. However, several challenges are still remaining on DED. For example, residual heat deteriorates shape accuracy during deposition. When depositing the higher layers as shown in Fig. 1(a), the top of deposited part anneals because the heat energy is hardly transferred to the baseplate across the lower layers with small cross-sectional area. As a result, the corner edge is rounded as shown in Fig. 1(b), and width increases in the high layers as shown in (c).

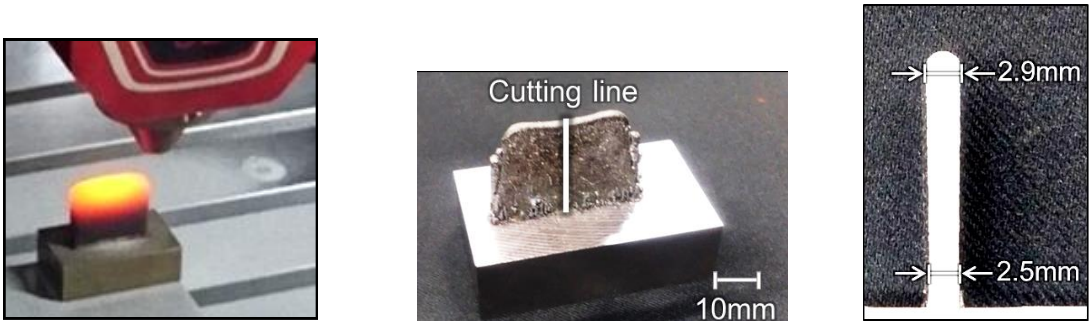

(a) Residual heat (b) Thin-wall deposited object (c) Cross section

Fig. 1 Deformation due to overheating in directed energy deposition

In order to suppress the deformation, the operators have to spend much time to find appropriate parameters for deposition by trial and error. Therefore, process optimization is a common issue in DED so that many researchers have focused on it until now. Manvatkar et al. conducted a heat transfer simulation to stabilize the DED process by analyzing the relation between the laser beam conditions and the meltpool shape [3]. Ahsan and Pinkerton proposed an analytical method for microstructure formation and clarified the influence of laser power and mass flow rate on the process stability [4]. Amine analyzed the reheating cycle in upper layer deposition based on a heat transfer model and theoretically showed that the cooling rate decreases at higher layers [5]. Although these proposals are effective to clarify the influence of deposition parameters, the process stability should be actively ensured by parameter modification according to the state of meltpool, which is estimated with the analytical approaches in advance.

Against these backgrounds, this study proposes a laser command generation for suppression of overheating in DED by applying a heat conduction simulation. The laser command is determined by a three-dimensional heat conduction simulation with a finite difference method and an inverse calculation. The proposed method sufficiently enhanced the shape accuracy by keeping the meltpool temperature constant during the deposition.

Methodology

Three-dimensional Heat Conduction Equation. In order to estimate temperature distribution in a deposited part, a time-domain simulation is conducted based on a three-dimensional heat conduction equation as follows:

$$c\rho\frac{\partial T}{\partial t} = K\left(\frac{\partial^2 T}{\partial x^2} + \frac{\partial^2 T}{\partial y^2} + \frac{\partial^2 T}{\partial z^2}\right) + q_v \tag{1}$$

where c [J/kg·K] is the specific heat, ρ [kg/m^3] is the density, T [K] is the instantaneous temperature, K [J/s·m·K] is the thermal conductivity, q_v [W] is the heat supply, t [s] is the time, and the subscripts x, y, and z are defining parameters in the spatial directions x, y, and z respectively. Considering a finite element model as shown in Fig. 2, heat transfer should be calculated in a discrete domain along with a central difference approximation as follows:

$$\frac{\partial^2 T}{\partial r^2} = \frac{T_{r+\Delta r} - 2T_r + T_{r-\Delta r}}{(\Delta r)^2}\ (r = x, y, z) \tag{2}$$

where Δx [mm], Δy [mm], and Δz [mm] are the element length, width, and height respectively.

Furthermore, the heat is supplied into the elements in the laser spot. For keeping the meltpool temperature constant, the heat supply in Eq. (1) is obtained by inverse calculation as follows:

$$q_v = \sum_{n=1}^{S} (T_{target} - T_n) \cdot c\rho \Delta x \Delta y \Delta z \quad (3)$$

where S is the number of elements under laser spot, T_{target} [K] is the target meltpool temperature, and T_n [K] is the present temperature of each element in the meltpool. The simulation parameters are summarized in Table 1.

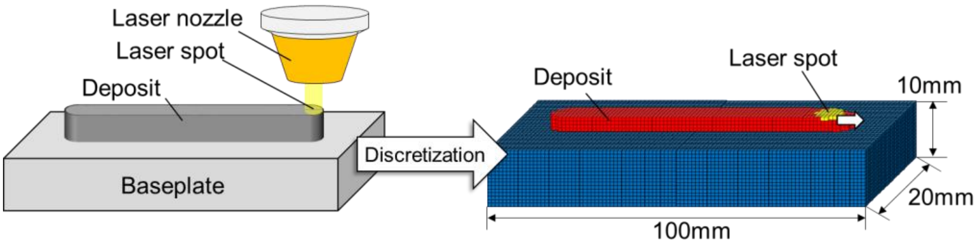

Fig. 2 Three-dimensional heat conduction simulation model

Table 1 Simulation parameters

Parameters		Inconel625	SUS304
Density	[kg/m^3]	8450	8030
Thermal conductivity	[J/s·m·K]	10.0	16.0
Specific heat	[J/kg·K]	410.0	500.0
Feed rate	[m/s]	0.0167	
Element size	[mm]	0.4×0.4×0.4	
Deposition length	[mm]	70	
Number of layer	-	20	
Layer height	[mm]	0.4	
Step time	[ms]	0.1	
Initial temperature	[℃]	25.0	
Meltpool temperature	[℃]	2500.0	
Meltpool diameter	[mm]	3.2	

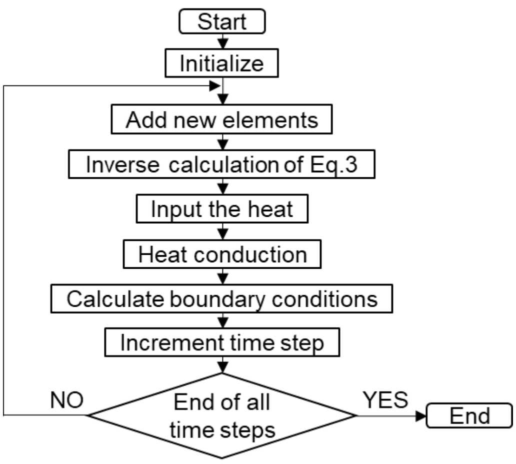

Fig. 3 Flowchart of proposal method

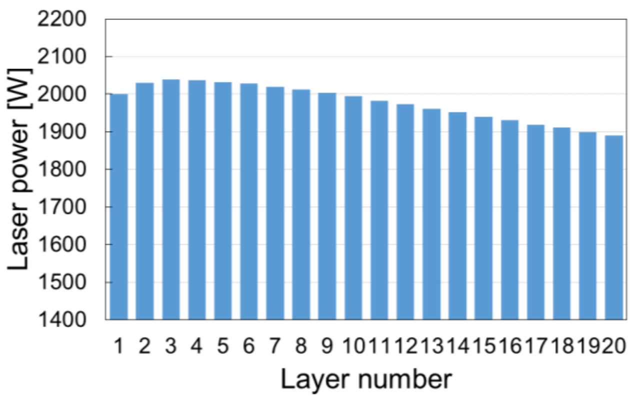

Fig. 4 Generated Laser command for each layer

Laser Command Generation. In order to keep the meltpool temperature constant, the required laser power is calculated at each time step along with the flowchart shown in Fig. 3. By calculating the average of required laser power at each layer, a proper laser command along with the number of layer is identified as shown in Fig. 4.

Experiment

Experiment Setup. Deposition tests were conducted by using a five-axial machining center (LASERTEC 65 3D, DMG MORI CO., LTD.), built-in DED function. Inconel 625 powder (grain size of 45 to 125 µm) and SUS304 baseplates are selected in this study. Fig. 5 shows the experimental apparatus. The deposition conditions are summarized in Table 2, and the deposition path is shown in Fig. 6. By repeating 20-layer deposition test with both a constant (2000 W) and the adjusted laser commands, the validity of proposed method was experimentally evaluated.

Table 2 Deposition conditions

Metal powder feed rate	[g/min]	18
Carrier gas feed rate	[l/min]	6
Shielding gas feed rate	[l/min]	4
Nozzle feed rate	[mm/min]	1000

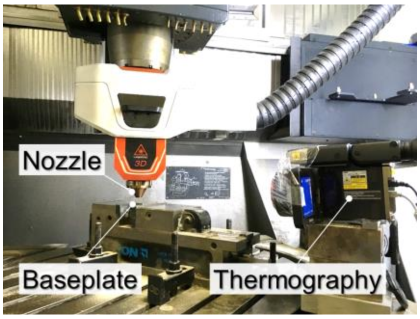

Fig. 5 Experimental setup

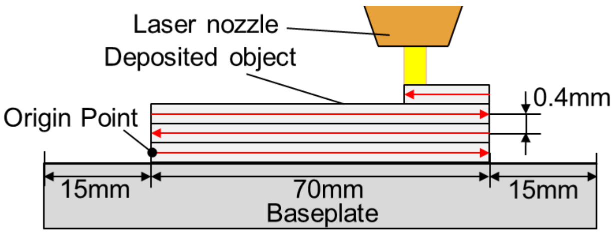

Fig. 6 Deposition trajectory for thin-wall deposited object

Validation of simulation model. An infrared thermography (InfReC R500EX-Pro, Nippon Avionics Co.,Ltd.) was employed for measuring the temperature distribution on the surface of deposited part. Fig. 7(a) and (b) show thermal images obtained by the proposed method and the measurement just after 20th layer deposition with laser power of 2000 W. Furthermore, Fig. 7(c) shows the comparison of analytical and measurement results of temperature distribution at top layer. Although the peak temperature is sharp under the laser spot in the simulation result, the temperature variation is small in the measurement result.

(a) Thermal image of simulation result

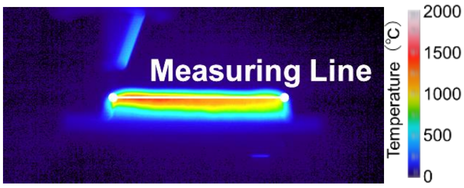

(b) Thermal image of experiment result

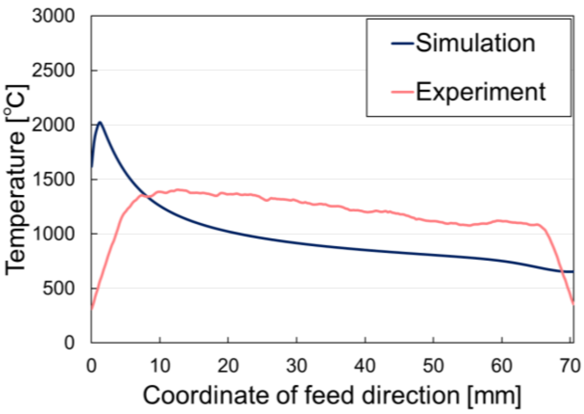

(c) Temperature distribution on the top surface

Fig. 7 Thermal image and temperature distribution after the 20th layer deposition

On the other hand, the analytical and measurement of temperature distributions are similar 0.6 seconds after finishing the deposition as shown in Fig. 8. From these results, the proposed method certainly has an ability to estimate the heat transfer at low temperature like in a solid phase. However, the developed simulation does not consider the changes in heat conductivity and emissivity at high temperature, i.e., in a liquid phase. In order to accurately estimate the thermal distribution in a high temperature condition, the simulation parameters should be modified along with the element temperature based on physical characteristics of molten metal.

(a) Thermal image of simulation result

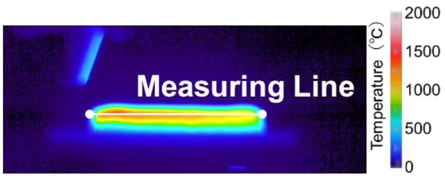

(b) Thermal image of experiment result

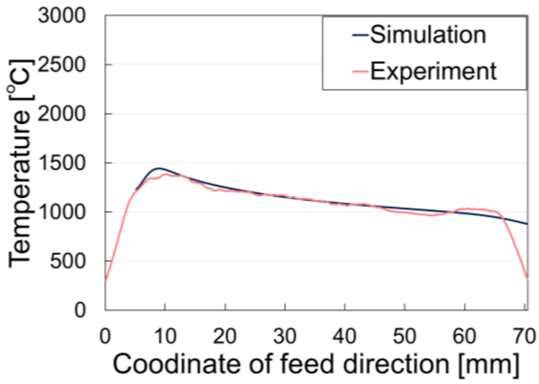

(c) Temperature distribution on the top surface

Fig. 8 Temperature distribution 0.6 seconds after finish of deposition

Evaluation Results in Shape Accuracy

30-mm long thin walls, which is the more deformable shape, were deposited with 8-mm height. The center of thin wall is cut with an abrasive jet cutter to observe the cross-section as shown in Fig. 9. The width measurement of deposit is summarized in Fig. 10 relating to the deposition height. As a result, the width expansion at top area was suppressed with the adjusted laser power. In order to evaluate the versatility of proposed method, deposition tests were also conducted on a 70-mm long track (Fig. 11) and a cylindrical track (Fig. 12). These results show that the deformation due to overheating can be efficiently suppressed by changing the laser power according to the thermal condition around the meltpool.

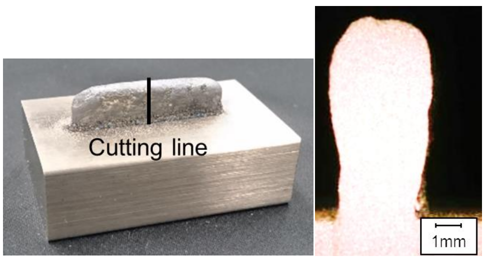

(a) Under the constant laser command

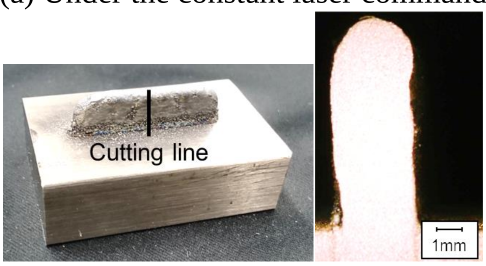

(b) Under the adjusted laser command

Fig. 9 30-mm long thin wall deposited objects and cross sections

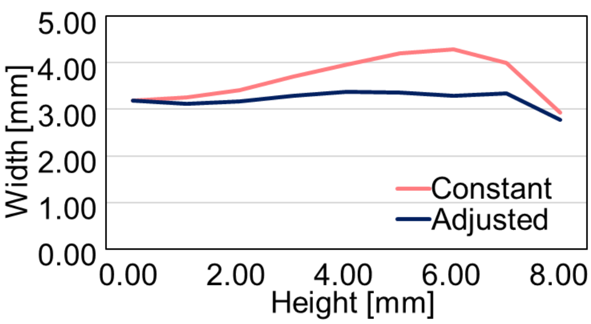

Fig. 10 Relation between width and height of thin wall deposited objects

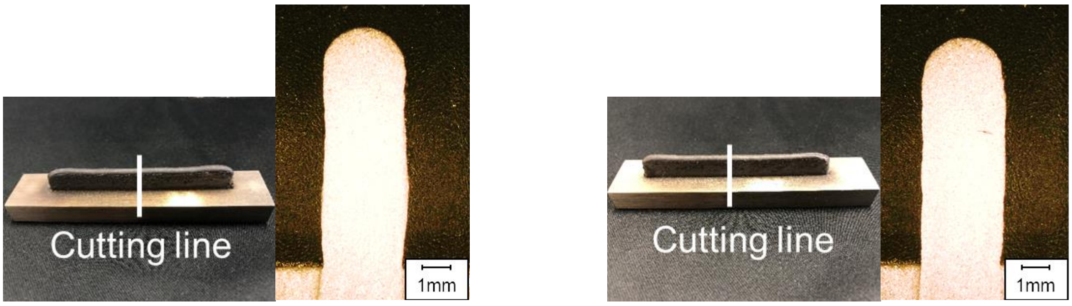

(a) Under the constant laser command (b) Under the adjusted laser command

Fig. 11 70-mm long thin wall deposited objects and cross sections

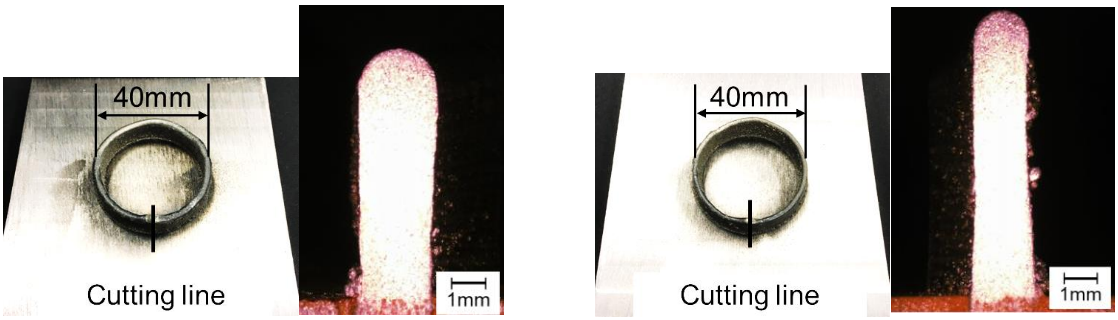

(a) Under the constant laser command (b) Under the adjusted laser command

Fig. 12 Cylinder deposited objects and cross sections

Summary

In order to suppress the deformation due to overheating in DED, this study proposes a laser command generation available to each deposition path by applying a heat conduction simulation and an inverse calculation. Compared with a conventional process with constant laser power, the proposed method successfully suppressed the width expansion at the top of deposit. The obtained results are summarized as follows:

1. The estimated result of temperature distribution 0.6 seconds after deposition certainly agrees with the measurement result obtained by thermography.
2. The differences between the simulation and the experiment results are considered to be due to the thermal characteristic change between the solid and liquid phases.
3. The propose method is available for various kinds of tracks to suppress the width expansion due to overheating.

References

[1] Standard Terminology for Additive Manufacturing Technologies, F2792-12a - Standard Terminology for Additive Manufacturing Technologies, ASTM Int. (2013) 10–12

[2] M. Schmidt, M. Merklein, D. Bourell, D. Dimitrov, T. Hausotte, K. Wegener, L. Overmeyer, F. Vollertsen, and G. N. Levy, Laser based additive manufacturing in industry and academia, CIRP Ann. 66 (2017) 561–583

[3] V. Manvatkar, A. De, and T. DebRoy, Spatial variation of melt pool geometry, peak temperature and solidification parameters during laser assisted additive manufacturing process, Mater. Sci. Technol. 31 (2015) 924–930

[4] M. N. Ahsan and A. J. Pinkerton, An analytical-numerical model of laser direct metal deposition track and microstructure formation, Model. Simul. Mater. Sci. Eng. 19 (2011)

[5] T. Amine, J. W. Newkirk, and F. Liou, Investigation of effect of process parameters on multilayer builds by direct metal deposition, Appl. Therm. Eng. 73 (2014) 498–509